# Loss of ciliary zonule protein hydroxylation and lens stability as a predicted consequence of biallelic *ASPH* variation

Owen M Siggs[a*], Emmanuelle Souzeau[a], Jamie E Craig[a]

[a]Department of Ophthalmology, Flinders University, Flinders Medical Centre, Adelaide, Australia

Correspondence to: Owen M. Siggs, Department of Ophthalmology, Flinders Medical Centre, 1 Flinders Drive, Bedford Park SA 5042, Australia; phone: +61 8 8404 2035; F: +61 8 8204 6722; email: owen.siggs@flinders.edu.au

## Abstract

**Purpose**: Stability of the crystalline lens requires formation of microfibril bundles and their higher-order structures of ciliary zonules. Trauma, malformation, or degeneration of the ciliary zonules can lead to dislocation or displacement of the lens, which in turn can cause transient or permanent loss of visual acuity. The purpose of this study was to identify the predicted substrates of ASPH, a 2-oxoglutarate- and $Fe^{2+}$-dependent hydroxylase, which may account for the lens instability phenotype of *ASPH*-associated syndromes.

**Methods**: A single proband of European ancestry with spherophakia and high myopia was subjected to exome sequencing. Proteins containing the ASPH hydroxylation motif were identified within the SwissProt protein database.

**Results**: We identified 105 putative substrates of ASPH-mediated hydroxylation in the human proteome, of which two (FBN1 and LTBP2) are associated with inherited ectopia lentis syndromes, and are essential for microfibril and ciliary zonule development.

**Conclusion**: Our results implicate ASPH-mediated hydroxylation in the formation of FBN1/LTBP2 microfibril bundles and competent ciliary zonules.

## Keywords

Traboulsi syndrome, ASPH, LTBP2, FBN1, ectopia lentis

## Introduction

Ectopia lentis is the dislocation or displacement of the crystalline lens, and can lead to significant refractive error, pupillary block with associated glaucoma, retinal damage, and in some instances, blindness. Ectopia lentis may be secondary to ocular trauma [1], but may be also be primary, in which case it is typically bilateral and associated with congenital weakness of the ciliary zonules which hold the lens in place. Marfan syndrome is the most common cause of primary ectopia lentis, and is associated with heterozygous variants in the fibrillin-1 gene (*FBN1*).

Traboulsi syndrome, also known as FDLAB syndrome (facial dysmorphism, lens dislocation, anterior-segment abnormalities, and spontaneous filtering blebs), is a rare ocular malformation syndrome associated with ectopia lentis [2,3,4,5,6]. FDLAB syndrome is caused by biallelic variants at the *ASPH* locus [5], which encodes at least three unique proteins: junctin, junctate, and aspartyl/asparaginyl hydroxylase (ASPH) [7]. All variants associated with FDLAB syndrome uniquely affect APSH, which encodes a 2-oxoglutarate-dependent oxygenase enzyme that catalyzes C-3 hydroxylation of aspartic acid and asparagine residues in the endoplasmic reticulum [8]. The 2-oxoglutarate-dependent oxygenases are a family of non-heme, $Fe^{2+}$-dependent enzymes, and include several essential regulators of oxygen homeostasis via the transcription factor HIF (hypoxia-inducible factor) [9].

With only five pedigrees and three pathogenic variants reported to date, there is little understanding of the phenotypic spectrum and mechanistic processes associated with biallelic variation in *ASPH*. We describe an individual with compound heterozygous *ASPH* variants, and explore the mechanism by which ASPH promotes lens stability.

## Material & Methods

*Human subjects*

Patients and family members provided written informed consent under protocols approved by the Southern Adelaide Clinical Human Research Ethics Committee (305-08).

*DNA sequencing and analysis*

DNA was prepared from whole blood and sequenced as previously described (Siggs et al. 2018, JAMA Ophthalmology, in press).

*Protein sequence analysis*

Protein sequences were aligned with Clustal Omega and BOXSHADE. Structural analysis was performed using PDB structure 5JQY in UCSF Chimera. Putative ASPH substrates were identified by searching the SwissProt database for the consensus hydroxylation motif (C-x-[DN]-x(4)-[FY]-x-C-x-C) in genome.jp/tools/motif/MOTIF2.html.

## Results

We identified a single individual who presented at 16 years of age with bilateral high myopia, shallow anterior chambers, spherophakia, and closed iridocorneal angles (Figure 1B-D). She was of non-consanguineous European ancestry, with no family history of early-onset eye

disease. Mild ocular hypertension was observed (maximum intraocular pressure of 23 mm Hg bilaterally), as were thin corneas (534/519 μm), and vertical cup:disc ratios were 0.6 bilaterally (Supplementary Table 1). Her facial appearance was remarkable for retrognathia and a beaked nose, and dental malocclusion (Figure 1E-F). She had no apparent cardiovascular or skeletal abnormalities, and was of average height.

To test for the presence of an underlying genetic cause of her condition, DNA isolated from peripheral blood was subjected to exome sequencing. We considered the subset of variants with a gnomAD r2.0.2 allele frequency < 0.0001. Of those variants predicted to be nonsense, essential splice, missense, frameshift, or in-frame insertions or deletions, 8 were compatible with a recessive mode of inheritance, including two rare coding variants of uncertain phase were identified in *ASPH*, both of which were predicted to be deleterious by PolyPhen2, SIFT, and CADD algorithms (Supplementary Table 2). Parental sequencing subsequently confirmed these variants to be *in trans* in the proband (Figure 2A, B). Given the phenotypic similarities of this patient with previously described cases of *ASPH*-associated disease [5], we considered these variants to be a likely explanation for the patient's phenotype.

Both variants (p.Cys641Ter and p.Arg735Gln) were located in the C-terminal catalytic domain of ASPH, which is unique to ASPH and absent from the junctin and junctate protein isoforms (Figure 2C). One of these variants (p.Cys641Ter) was a premature termination codon and predicted loss-of-function allele, while the second (p.Arg735Gln) was a missense substitution at a critical catalytic domain residue. A different substitution at the same residue (p.Arg735Trp) was reported in homozygous form in two Lebanese individuals with FDLAB syndrome [3–5].

Arg735 is conserved across vertebrates and invertebrates (Figure 2E), and forms two critical salt bridges with an essential cofactor (2-oxoglutarate). 2-oxoglutarate in turn helps coordinate a catalytic $Fe^{2+}$ ion, and recruitment of the aspartic acid or asparagine substrate for hydroxylation (Figure 2F). As is the case with p.Arg735Trp, p.Arg735Gln is predicted to abolish 2-oxoglutarate binding, and therefore eliminate all catalytic activity of ASPH.

ASPH hydroxylates aspartic acid and asparagine substrates within a defined consensus motif (C-x-[DN]-x(4)-[FY]-x-C-x-C) [10]. We searched the SwissProt database for all human proteins containing the ASPH hydroxylation motif, revealing 105 putative targets (Supplementary Table 3). These included the vitamin K-dependent coagulation factors VII, IX, X, protein C, and protein S; the low- and very low-density lipoprotein receptors; thyroid peroxidase (TPO); complement components C1R and C1S; and ligands (JAG1, JAG2) and receptors (NOTCH1-4) of the Notch family. Measurements of coagulation, lipoprotein homeostasis, thyroid function, and the complement cascade were all within normal limits in peripheral blood samples from the proband (Supplementary Table 4), suggesting that ASPH hydroxylation may be physiologically redundant in these settings.

There were two predicted ASPH substrates, latent transforming growth factor beta binding protein-2 (LTBP2) and fibrillin-1 (FBN1), which were of particular interest, given that variants in the genes encoding them are associated with Mendelian syndromes with stark phenotypic similarities to FDLAB syndrome. Heterozygous variants in *FBN1* cause Marfan syndrome: a common cause of primary ectopia lentis [11]. Similarly, homozygous or compound heterozygous

variation in *LTBP2* is associated with microspherophakia, ectopia lentis, and in some instances, with secondary glaucoma [12–14]. FBN1 and LTBP2 have two of highest numbers of predicted ASPH hydroxylation sites, at 43 and 13 sites respectively (Figure 3A). All of these motifs fall within EGF-like domains, and all but one are of the calcium-binding EGF-like (cbEGF) subtype (Figure 3B).

## Discussion

We provide evidence that biallelic ASPH variants can be associated with a unique syndrome of spherophakia, high myopia, shallow anterior chambers, and a distinct facial appearance. The individual described in this study had not developed ectopia lentis, iris atrophy, or spontaneous filtering blebs by the age of 17, making her presentation distinct from classical FDLAB syndrome, although these features may still emerge with age, particularly given that spherophakia often precedes ectopia lentis. Dental malocclusion had been described previously [2,3], and in this case manifested as a maxillary ectopic canine. Of note is the association with cholesteatoma, often associated with craniofacial abnormalities, although not described previously in *ASPH*-associated disease.

Of the 105 putative ASPH substrates identified here, the closest phenotypic overlap is with LTBP2 and FBN1, both of which are associated with Mendelian syndromes with ocular and lenticular phenotypes. Importantly, other proteins implicated in syndromic or isolated forms ectopia lentis (ADAMTSL4, ADAMTS10, and ADAMTS17) did not harbor the ASPH consensus hydroxylation motif, indicating that ASPH has a much narrower substrate specificity than previously expected [5].

LTBP2 and FBN1 are interacting members of the LTBP-fibrillin extracellular matrix (ECM) glycoprotein superfamily, sharing 25% homology, and bind directly to one another in a calcium-dependent manner [15]. Their domain structure is rich in calcium-binding epidermal growth factor-like (cbEGF) domains, interspersed with TGF-β binding protein-like (TB) domains. FBN1 is a key structural component of extracellular microfibrils present in the skin, lung, kidney, vasculature, cartilage, tendon, muscle, cornea, and ciliary zonule [16], while both FBN1 and LTBP2 act in unison to support formation of ciliary zonules [17]. Asparagine hydroxylation has been observed in FBN1 extracted from human amnion [18], although the functional significance of hydroxylation is yet to be determined.

Our data suggest that ASPH-associated lenticular abnormalities, and perhaps other phenotypes, are secondary to reduced hydroxylation of LTBP2 and/or FBN1, which in turn disrupts microfibril formation, ciliary zonule structure, and ultimately reduce stability of the lens [17].

## Acknowledgements

We thank Angela Chappell and Carly Emerson for photography. Supported by the Channel 7 Children's Research Foundation, and the Australian National Health & Medical Research Council (NHMRC, Centres of Research Excellence Grant 1116360, Project Grant APP1107098). JEC was an NHMRC Practitioner Fellow. The authors declare no conflict of interest.

**References**


1. Jarrett WH. Dislocation of the Lens: A Study of 166 Hospitalized Cases. *Arch Ophthalmol*. 1967;78(3):289.

2. Shawaf S, Noureddin B, Khouri A, Traboulsi EI. A family with a syndrome of ectopia lentis, spontaneous filtering blebs, and craniofacial dysmorphism. *Ophthalmic Genet*. 1995;16(4):163-169.

3. Haddad R, Uwaydat S, Dakroub R, Traboulsi EI. Confirmation of the autosomal recessive syndrome of ectopia lentis and distinctive craniofacial appearance. *Am J Med Genet*. 2001;99(3):185-189.

4. Mansour AM, Younis MH, Dakroub RH. Anterior segment imaging and treatment of a case with syndrome of ectopia lentis, spontaneous filtering blebs, and craniofacial dysmorphism. *Case Rep Ophthalmol*. 2013;4(1):84-90.

5. Patel N, Khan AO, Mansour A, et al. Mutations in ASPH cause facial dysmorphism, lens dislocation, anterior-segment abnormalities, and spontaneous filtering blebs, or Traboulsi syndrome. *Am J Hum Genet*. 2014;94(5):755-759.

6. Abarca Barriga HH, Caballero N, Trubnykova M, et al. A novel ASPH variant extends the phenotype of Shawaf-Traboulsi syndrome. *Am J Med Genet A*. September 2018. doi:10.1002/ajmg.a.40508

7. Treves S, Feriotto G, Moccagatta L, Gambari R, Zorzato F. Molecular cloning, expression, functional characterization, chromosomal localization, and gene structure of junctate, a novel integral calcium binding protein of sarco(endo)plasmic reticulum membrane. *J Biol Chem*. 2000;275(50):39555-39568.

8. Islam MS, Leissing TM, Chowdhury R, Hopkinson RJ, Schofield CJ. 2-Oxoglutarate-Dependent Oxygenases. *Annu Rev Biochem*. March 2018. doi:10.1146/annurev-biochem-061516-044724

9. Schofield CJ, Ratcliffe PJ. Oxygen sensing by HIF hydroxylases. *Nat Rev Mol Cell Biol*. 2004;5(5):343-354.

10. Stenflo J, Ohlin AK, Owen WG, Schneider WJ. beta-Hydroxyaspartic acid or beta-hydroxyasparagine in bovine low density lipoprotein receptor and in bovine thrombomodulin. *J Biol Chem*. 1988;263(1):21-24.

11. Pyeritz RE, McKusick VA. The Marfan syndrome: diagnosis and management. *N Engl J Med*. 1979;300(14):772-777.

12. Désir J, Sznajer Y, Depasse F, et al. LTBP2 null mutations in an autosomal recessive ocular syndrome with megalocornea, spherophakia, and secondary glaucoma. *Eur J Hum Genet*. 2010;18(7):761-767.

13. Kumar A, Duvvari MR, Prabhakaran VC, Shetty JS, Murthy GJ, Blanton SH. A homozygous mutation in LTBP2 causes isolated microspherophakia. *Hum Genet*. 2010;128(4):365-371.

14. Khan AO, Aldahmesh MA, Alkuraya FS. Congenital megalocornea with zonular weakness and childhood lens-related secondary glaucoma - a distinct phenotype caused by recessive

LTBP2 mutations. *Mol Vis*. 2011;17:2570-2579.

15. Hirani R, Hanssen E, Gibson MA. LTBP-2 specifically interacts with the amino-terminal region of fibrillin-1 and competes with LTBP-1 for binding to this microfibrillar protein. *Matrix Biol*. 2007;26(4):213-223.

16. Sakai LY. Fibrillin, a new 350-kD glycoprotein, is a component of extracellular microfibrils. *J Cell Biol*. 1986;103(6):2499-2509.

17. Inoue T, Ohbayashi T, Fujikawa Y, et al. Latent TGF-β binding protein-2 is essential for the development of ciliary zonule microfibrils. *Hum Mol Genet*. 2014;23(21):5672-5682.

18. Glanville RW, Qian RQ, McClure DW, Maslen CL. Calcium binding, hydroxylation, and glycosylation of the precursor epidermal growth factor-like domains of fibrillin-1, the Marfan gene protein. *J Biol Chem*. 1994;269(43):26630-26634.

**Figure 1. Craniofacial and anterior segment dysgenesis phenotypes associated with biallelic *ASPH* variants**

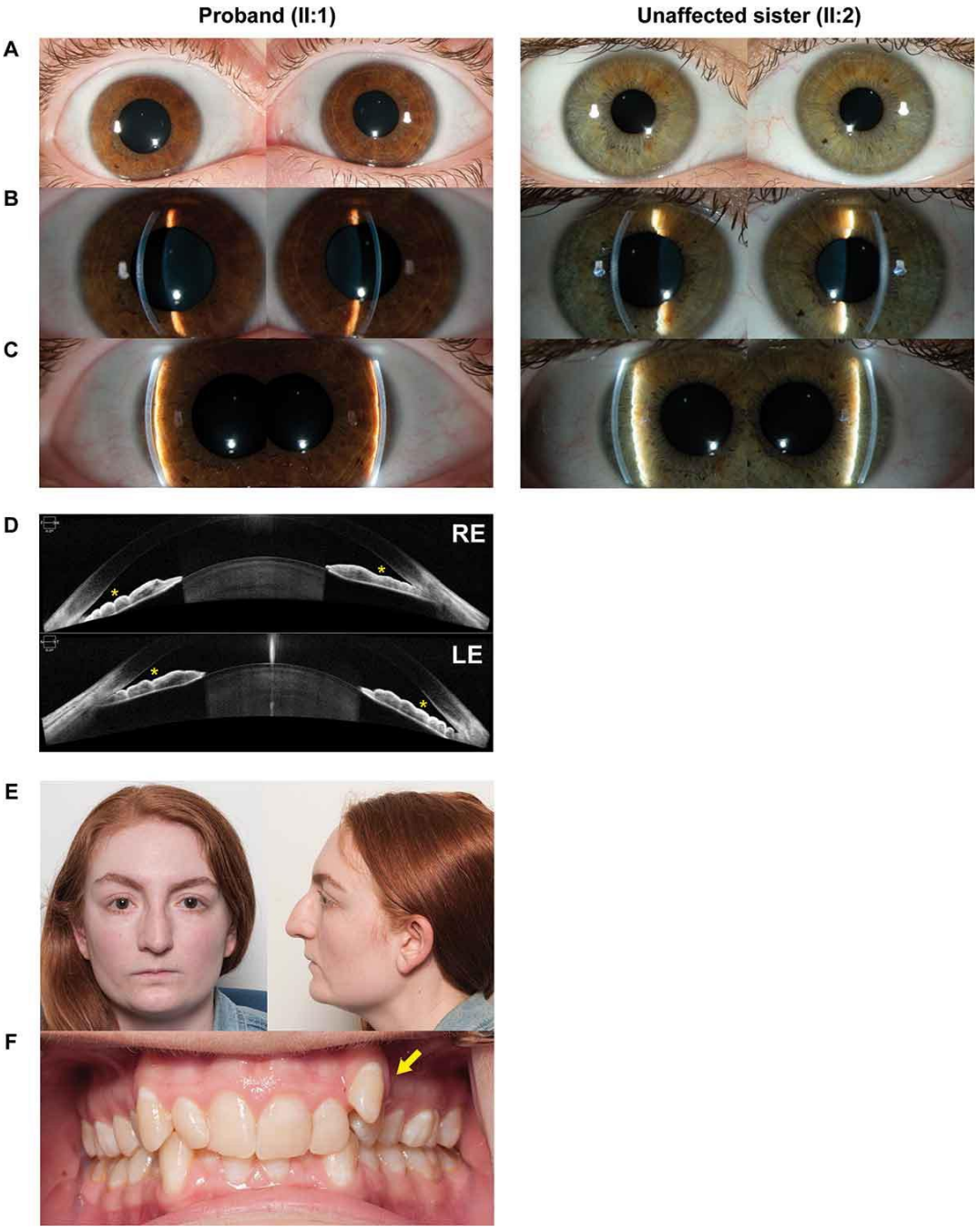


Slit lamp examination of the proband (left panels) and her unaffected sister (right panels) revealed mid-dilatation of both pupils (A), and bilateral shallow central (B) and peripheral (C) anterior chambers in the proband. Anterior segment optical coherence tomography (D) revealed bilateral spherophakia, anterior iris convexity, an anterior lens vault, and iridocorneal apposition (yellow asterisks). Portrait and profile of the proband (E), with images of a maxillary ectopic canine (F, yellow arrow).

**Figure 2. Biallelic *ASPH* variants**

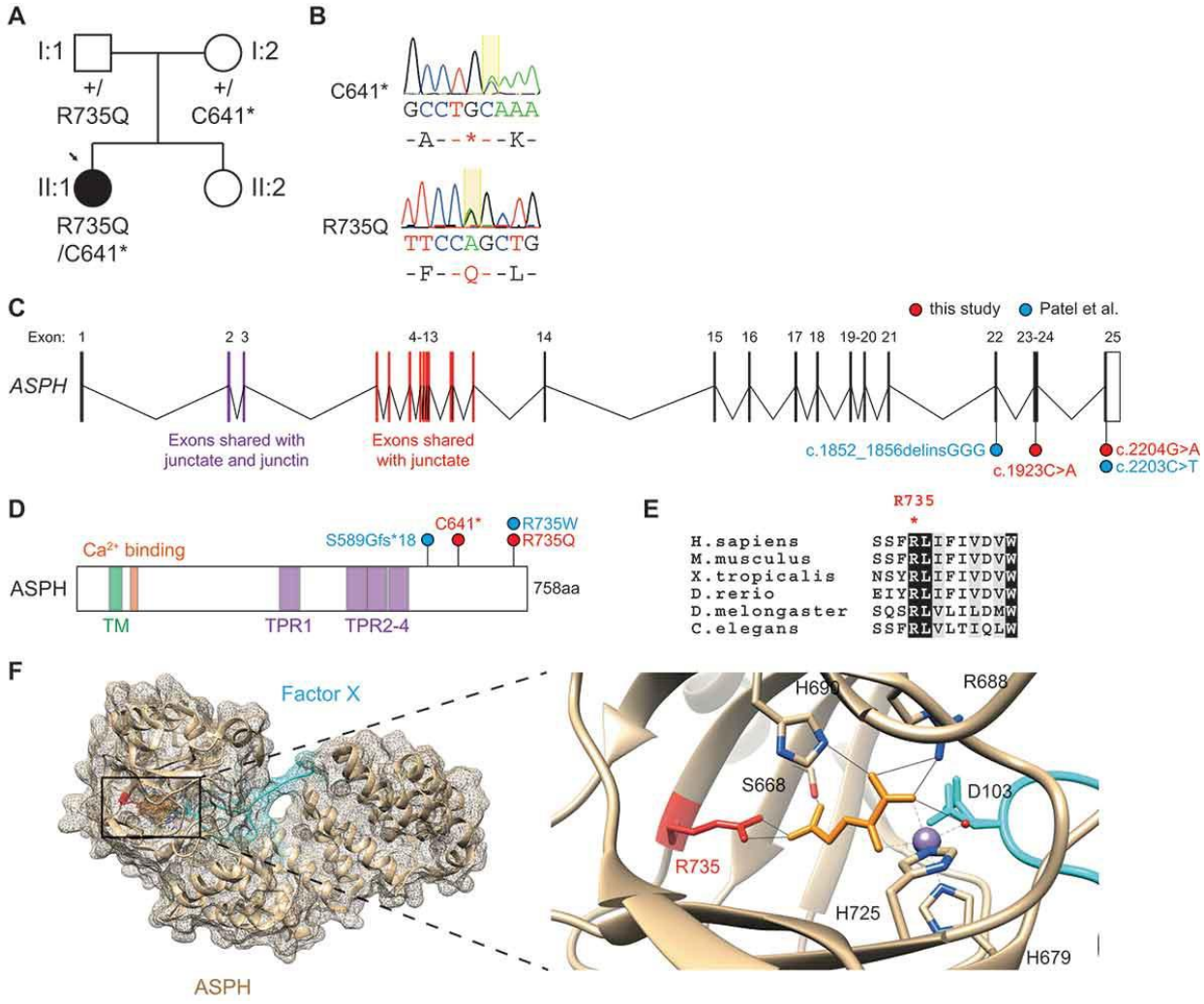


(A) Pedigree of the family described in this study. Round symbols indicate females; square symbols, males; black symbols, affected; arrow, proband; +, reference allele.
(B) Sanger sequencing traces
(C) *ASPH* locus and position of disease-associated variants described in this study, and others [5]. Exons shared with the junctate and junctin isoforms are highlighted in purple or red.
(D) ASPH protein schematic and domain structure, showing location of disease-associated missense, nonsense, and frameshift variants. TM, transmembrane domain; TPR, tetratricopeptide repeat.
(E) ASPH protein sequence alignments across multiple model organisms. Arginine 735 is highlighted.
(F) X-ray crystal structure of ASPH with Factor X peptide (PDB: 5JQY). Active site magnified, showing Arginine 735 (red), manganese ion (purple), N-oxalylglycine (yellow), and Factor X peptide with aspartate substrate (blue).

**Figure 3. Predicted ASPH substrates and hydroxylation motif density**

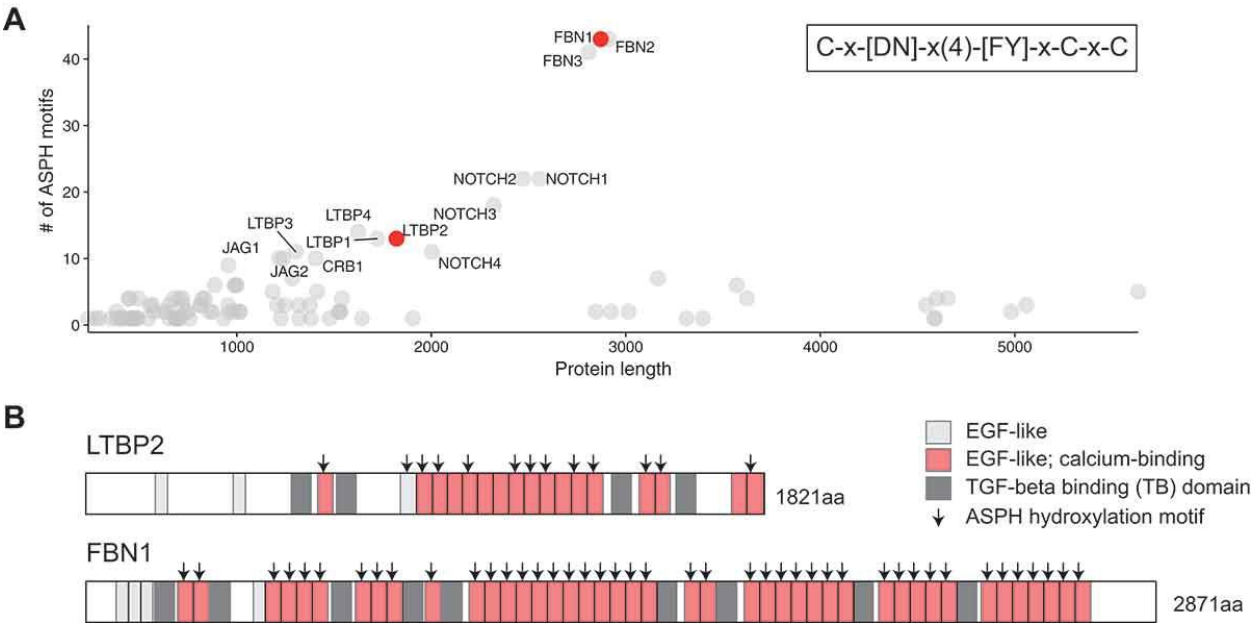


(A) Abundance of ASPH consensus hydroxylation mofits (C-x-[DN]-x(4)-[FY]-x-C-x-C) within 105 human proteins. Proteins with 10 or more motifs are labelled, and those implicated in Mendelian ectopia lentis conditions are highlighted in red.
(B) Domain architecture of LTBP2 and FBN1 proteins, indicating the location of the ASPH consensus hydroxylation mofit (arrows). All but one of these motifs are located in calcium-binding EGF-like domains.

**Supplementary Data**

**Supplementary Table 1. Clinical details of proband with compound heterozygous *ASPH* variants**

RE, right eye; LE, left eye; BCVA, best corrected visual acuity; AC, anterior chamber; IOP, intraocular pressure; CCT, central corneal thickness; PI, peripheral iridotomy.

| | **Family 1** | | | |
|---|---|---|---|---|
| **ID** | II:1 | | II:2 | |
| **Sex** | F | | F | |
| **Ancestry** | European | | European | |
| **Consanguinity** | no | | no | |
| **Age at diagnosis (y)** | 16 | | - | |
| **Age at last follow-up (y)** | 18 | | 23 | |
| **Facial dysmorphism** | beaked nose, retrognathia | | - | |
| **Dental malocclusion** | left maxillary ectopic canine | | - | |
| **Other features** | dermoid cyst, cholesteatoma, | | - | |
| | posterior fossa arachnoid cysts | | | |
| **Eye** | RE | LE | RE | LE |
| **BCVA** | 6/7.6 | 6/9.5 | 6/6 | 6/6 |
| **Refraction (D)** | -4.50 | -6.00 | +0.25 | -0.50 |
| **AC depth (mm)** | 2.17 | 2.16 | - | - |
| **Ectopia lentis** | no | no | - | - |
| **Spherophakia** | yes | yes | - | - |
| **Filtering blebs** | no | no | - | - |
| **Corectopia** | no | no | - | - |
| **Iris stromal hypoplasia** | no | no | - | - |
| **Iris transillumination** | no | no | - | - |
| **Iridocorneal angle** | closed | closed | - | - |
| **Posterior embryotoxon** | no | no | - | - |
| **Vertical cup:disc ratio** | 0.6 | 0.6 | 0.5 | 0.5 |
| **Max IOP (mm Hg)** | 23 | 23 | 15 | 16 |
| **CCT (um)** | 534 | 519 | 557 | 552 |
| **Axial length (mm)** | 22.03 | 22.43 | 23.44 | 23.49 |
| **Surgery** | PI | PI | - | - |

**Supplementary Table 2. *ASPH* variants associated with anterior segment dysgenesis phenotype**

Position of each predicted pathogenic variant with the human genome (hg19 reference), consensus transcript (NM_004318), and protein (NP_004309) described using HGVS nomenclature (version 15.11). Frequencies of each allele in the gnomAD r2.0.2 database is shown, as are CADD, PolyPhen-2, and SIFT scores with predictions of deleteriousness. AF, allele frequency; D, deleterious; T, tolerated.

| gDNA (hg19) | cDNA (NM_004318) | exon | protein (NP_004309) | gnomAD r2.0.2 AF | CADD_phred | PP2_HVAR | SIFT |
|---|---|---|---|---|---|---|---|
| g.8:62430660C>A | c.1836C>A | 23 | p.Cys641Ter | . | 37 | . | . |
| g.8:62415991G>A | c.2117G>A | 25 | p.Arg735Gln | 4/242206 (0.00001651) | 35 | 1; D | 0.018; D |

**Supplementary Table 3. Putative substrates of ASPH**

Genomic coordinates (hg19), associated human phenotypes and mouse orthologs, and numbers of predicted hydroxylation motifs in each full-length protein.

| Symbol | Ensembl Gene ID | Length | ASPH motifs |
|---|---|---|---|
| ADGRE1 | ENSG00000174837 | 886 | 6 |
| ADGRE2 | ENSG00000127507 | 823 | 4 |
| ADGRE3 | ENSG00000131355 | 652 | 1 |
| ADGRE4P | ENSG00000268758 | 457 | 1 |
| ADGRE5 | ENSG00000123146 | 835 | 4 |
| ADGRL4 | ENSG00000162618 | 690 | 1 |
| BMP1 | ENSG00000168487 | 986 | 2 |
| C1R | ENSG00000159403 | 705 | 1 |
| C1S | ENSG00000182326 | 688 | 1 |
| CCBE1 | ENSG00000183287 | 406 | 1 |
| CD248 | ENSG00000174807 | 757 | 1 |
| CD93 | ENSG00000125810 | 652 | 3 |
| CELSR1 | ENSG00000075275 | 3014 | 2 |
| CELSR2 | ENSG00000143126 | 2923 | 2 |
| CELSR3 | ENSG00000008300 | 3312 | 1 |
| CLEC14A | ENSG00000176435 | 490 | 1 |
| CRB1 | ENSG00000134376 | 1406 | 10 |
| CRB2 | ENSG00000148204 | 1285 | 7 |

| | | | |
|---|---|---|---|
| CRELD1 | ENSG00000163703 | 420 | 1 |
| CRELD2 | ENSG00000184164 | 353 | 1 |
| CUBN | ENSG00000107611 | 3623 | 4 |
| DLK1 | ENSG00000185559 | 383 | 1 |
| DLK2 | ENSG00000171462 | 383 | 2 |
| DLL1 | ENSG00000198719 | 723 | 3 |
| DLL4 | ENSG00000128917 | 685 | 1 |
| DNER | ENSG00000187957 | 737 | 2 |
| EDIL3 | ENSG00000164176 | 480 | 1 |
| EFEMP1 | ENSG00000115380 | 493 | 4 |
| EFEMP2 | ENSG00000172638 | 443 | 4 |
| EGF | ENSG00000138798 | 1207 | 3 |
| EGFL6 | ENSG00000198759 | 553 | 3 |
| EGFL7 | ENSG00000172889 | 273 | 1 |
| EGFL8 | ENSG00000241404 | 293 | 1 |
| EYS | ENSG00000188107 | 3165 | 7 |
| F10 | ENSG00000126218 | 488 | 1 |
| F7 | ENSG00000057593 | 466 | 1 |
| F9 | ENSG00000101981 | 461 | 1 |
| FAT1 | ENSG00000083857 | 4588 | 1 |
| FAT3 | ENSG00000165323 | 4589 | 1 |
| FAT4 | ENSG00000196159 | 4981 | 2 |
| FBLN1 | ENSG00000077942 | 703 | 4 |
| FBLN2 | ENSG00000163520 | 1184 | 5 |
| FBLN5 | ENSG00000140092 | 448 | 4 |
| FBLN7 | ENSG00000144152 | 439 | 1 |
| FBN1 | ENSG00000166147 | 2871 | 43 |
| FBN2 | ENSG00000138829 | 2912 | 43 |
| FBN3 | ENSG00000142449 | 2809 | 41 |
| GAS6 | ENSG00000183087 | 721 | 4 |
| HEG1 | ENSG00000173706 | 1381 | 1 |
| HMCN1 | ENSG00000143341 | 5635 | 5 |
| HMCN2 | ENSG00000148357 | 5059 | 3 |
| JAG1 | ENSG00000101384 | 1218 | 10 |

| | | | |
|---|---|---|---|
| JAG2 | ENSG00000184916 | 1238 | 10 |
| LDLR | ENSG00000130164 | 860 | 2 |
| LRP1 | ENSG00000123384 | 4544 | 3 |
| LRP1B | ENSG00000168702 | 4599 | 4 |
| LRP2 | ENSG00000081479 | 4655 | 4 |
| LRP4 | ENSG00000134569 | 1905 | 1 |
| LRP8 | ENSG00000157193 | 963 | 2 |
| LTBP1 | ENSG00000049323 | 1721 | 13 |
| LTBP2 | ENSG00000119681 | 1821 | 13 |
| LTBP3 | ENSG00000168056 | 1303 | 11 |
| LTBP4 | ENSG00000090006 | 1624 | 14 |
| MASP1 | ENSG00000127241 | 699 | 1 |
| MASP2 | ENSG00000009724 | 686 | 1 |
| MATN2 | ENSG00000132561 | 956 | 9 |
| MATN4 | ENSG00000124159 | 622 | 2 |
| MEGF6 | ENSG00000162591 | 1541 | 4 |
| MEGF8 | ENSG00000105429 | 2845 | 2 |
| MMRN1 | ENSG00000138722 | 1228 | 1 |
| NCAN | ENSG00000130287 | 1321 | 1 |
| NELL1 | ENSG00000165973 | 810 | 3 |
| NELL2 | ENSG00000184613 | 816 | 3 |
| NID1 | ENSG00000116962 | 1247 | 3 |
| NID2 | ENSG00000087303 | 1375 | 3 |
| NOTCH1 | ENSG00000148400 | 2555 | 22 |
| NOTCH2 | ENSG00000134250 | 2471 | 22 |
| NOTCH2NL | ENSG00000213240 | 236 | 1 |
| NOTCH3 | ENSG00000074181 | 2321 | 18 |
| NOTCH4 | ENSG00000204301 | 2003 | 11 |
| NPNT | ENSG00000168743 | 565 | 3 |
| NRXN1 | ENSG00000179915 | 1477 | 1 |
| NRXN3 | ENSG00000021645 | 1643 | 1 |
| OIT3 | ENSG00000138315 | 545 | 1 |
| PROC | ENSG00000115718 | 461 | 1 |
| PROS1 | ENSG00000184500 | 676 | 4 |

| | | | |
|---|---|---|---|
| PROZ | ENSG00000126231 | 400 | 1 |
| SCUBE1 | ENSG00000159307 | 988 | 6 |
| SCUBE2 | ENSG00000175356 | 999 | 6 |
| SCUBE3 | ENSG00000146197 | 993 | 6 |
| SLIT1 | ENSG00000187122 | 1534 | 2 |
| SLIT2 | ENSG00000145147 | 1529 | 2 |
| SLIT3 | ENSG00000184347 | 1523 | 2 |
| SNED1 | ENSG00000162804 | 1413 | 5 |
| SUSD1 | ENSG00000106868 | 747 | 2 |
| SVEP1 | ENSG00000165124 | 3571 | 6 |
| THBD | ENSG00000178726 | 575 | 2 |
| TLL1 | ENSG00000038295 | 1013 | 2 |
| TLL2 | ENSG00000095587 | 1015 | 2 |
| TPO | ENSG00000115705 | 933 | 1 |
| UMOD | ENSG00000169344 | 640 | 2 |
| UMODL1 | ENSG00000177398 | 1318 | 3 |
| VCAN | ENSG00000038427 | 3396 | 1 |
| VLDLR | ENSG00000147852 | 873 | 2 |
| VWCE | ENSG00000167992 | 955 | 3 |

**Supplementary Table 4. Clinical analytes associated with predicted ASPH substrates**
Predicted ASPH substrates and their relevant clinical analytes as measured in the *ASPH* compound heterozygous proband at last follow-up (aged 18 years). Units and laboratory normal ranges are shown for reference.

| **Predicted ASPH substrate(s)** | **Analyte** | **Value** | **Units** | **Normal range** |
|---|---|---|---|---|
| F7, F9, F10, PROC, PROS1 | Prothrombin time | 15 | s | (12-16) |
| | Prothrombin INR | 1.2 | ratio | (0.9-1.2) |
| | Activated partial thromboplastin time | 34 | s | (24-38) |
| TPO | Thyroid stimulating hormone | 0.95 | mIU/L | (0.50-4.50) |
| | Free T4 | 18 | pmol/L | (10-20) |
| | Free T3 | 5.1 | pmol/L | (3.1-5.4) |
| | Thyroid peroxidase antibody | <5 | IU/mL | (<=49) |
| LDLR | HDL cholesterol | 1.4 | mmol/L | (1.0-2.2) |

| | | | | |
|---|---|---|---|---|
| | LDL cholesterol | 2.2 | mmol/L | (0.0-3.7) |
| | non-HDL cholesterol | 2.6 | mmol/L | |
| | Total:HDL cholesterol | 2.9 | ratio | (0.0-5.0) |
| | Total triglycerides | 0.9 | mmol/L | (0.3-2.0) |
| (Complete blood count) | Hemoglobin | 129 | g/L | (115-155) |
| | White cell count | 7.8 | x10e9/L | (4.0-11.0) |
| | Platelet count | 498 | x10e9/L | (150-450) |
| | Red blood cells | 4.72 | x10e12/L | (3.8-5.2) |
| | Neutrophils | 4.5 | x10e9/L | (1.8-7.5) |
| | Lymphocytes | 2.6 | x10e9/L | (1.5-3.5) |
| | Monocytes | 0.53 | x10e9/L | (0.2-0.8) |
| | Eosinophils | 0.1 | x10e9/L | (0.02-0.5) |
| | Basophils | 0.02 | x10e9/L | (<=0.10) |